Influence of electrode resistance on tunnel junction conductance

T. Will and R. Escudero
Instituto de Investigaciones en Materiales, Apartado Postal 70-360, México 20, D. F., México

(Received 27 March 1980; accepted for publication 6 October 1980)

The tunneling conductance of thin-film M-O-M junctions is distorted by electrode resistance, which can be significant if one of the electrodes is, for example, a semimetal. We present a model relating the tunneling conductance of junctions in which such resistance is appreciable with that of junctions in which it is negligible and comparison is made with experimental results in Al-oxide-Bi junctions. We conclude that much of the apparent variation in characteristics of such junctions is due to the distortion produced by the semimetal film.

PACS numbers: 73.40.Gk, 73.40.Rw

INTRODUCTION

Attempts to interpret the tunneling conductance of thin-film metal-oxide-semimetal (M-O-SM) junctions in terms of the band structure of the semimetal[1,2] have been made since at least 1967.[3–9] However, it has not been possible to associate unequivocally structure in the tunneling spectra with that in $E(\mathbf{k})$, although empirical correlations have occasionally been acceptable.

Two factors have impeded the use of tunneling as a reliable tool for verifying certain aspects of band-structure calculations, despite the optimistic results presented intially by Esaki and Stiles[10] for junctions in which the semimetal (SM) electrode is a monocrystal. The wide variability of the experimental tunneling conductance, commented or implied by a number of authors, has raised the question of whether in these junctions band-structure effects are predominant.[6,11] In addition, a dependable theory has yet to be developed which would support the desired detailed correlation between structure in the tunneling conductance with that in $E(\mathbf{k})$.[12]

We find that the finite resistance of the thin-film semimetal electrode distorts the tunneling conductance in M-O-SM junctions,[13] even when measured in a four-terminal configuration, and accounts for a significant part of the troublesome variability in experimental results. In all our "well-formed" junctions, that is in junctions whose conductance at 77 K resembles the letter W with clearly defined peak and valleys, the principal features occur reproducibly at certain energies once the distortion produced by the finite film resistance is compensated.

We present here the model used to compute the distortion of the tunneling characteristics brought about by the finite resistance of one of the electrodes. We then test the model experimentally in well-formed junctions of Al-Al_xO_y-Bi and show the overall consistency of the data once the distortion is compensated.

THE MODEL

The planar thin-film junction (Fig. 1) can be represented by an essentially one-dimensional model (Fig. 2) if one of the electrodes is resistanceless. In this scheme we represent the junction by a parallel configuration of N elemental junctions intercalated with resistances which together reflect the film resistance. We suppose laminar current flow and ignore the typically small capacitive reactance of the jucntion.[5] In usual experimental conditions the semimetal electrode is uniform and its resistivity is constant.

In accordance with the bridge/modulation techniques in use in many laboratories,[14–16] we assume that the total current in the junction is $I + i\cos\omega t$, where I is the current producing the junction polarization and i the ac sensing current (maintained constant despite junction nonlinearity). The polarization current is swept slowly. In the usual experimental configuration, currentless contacts are made at one extreme of the junction in order to measure the bias voltage $V(I)$ and the rms voltages $B_\omega(V)$ at frequency ω and $B_{2\omega}(V)$ at 2ω. The differential conductance of the junction, $\sigma(V) = dI/dV$, is related to $B_\omega(V)^{-1}$ and can be calibrated directly by substituting for the junction a decade resistance. Schemes also exist for calibrating indirectly $B_{2\omega}(V)$, which is proportional to d^2V/dI^2 and from which $d\sigma(V)/dV$ can be determined.[17]

In applying the model to an actual junction it will be necessary to relate electrode resistance (excluding that part which makes contact to the junction) r_E to the elemental resistance r intercalated between adjacent elemental junctions: $r = r_E/(N-1)$. Furthermore, the elemental differential resistance of each elemental junction will be $D(V) = N\Delta(V)$, evaluated at the appropriate local polariza-

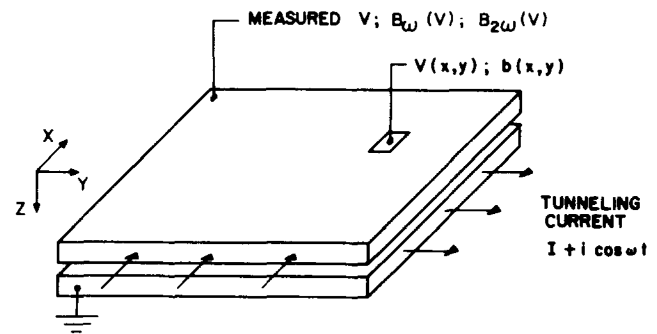

FIG. 1. Representation of a planar tunnel junction. The tunneling current produces dc and ac voltages, $V(x,y)$ and $b(x,y)$, respectively, which vary over the junction area because of electrode resistance. If only one electrode has appreciable resistance these voltages depend only on x. Currentless contacts are made at one extreme of the junction to measure the rms voltages $B_\omega(V)$ and $B_{2\omega}(V)$ at bias V.

 0021-8979/81/1405-06$01.10 © 1981 American Institute of Physics

Downloaded 18 Apr 2005 to 132.239.73.201. Redistribution subject to AIP license or copyright, see http://jap.aip.org/jap/copyright.jsp

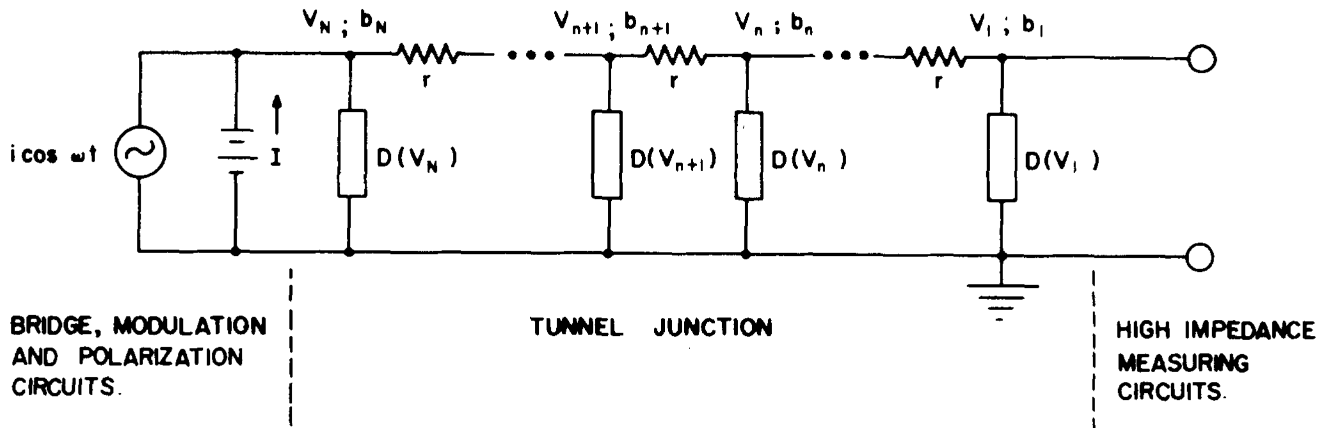

FIG. 2. Model of N elements representing planar tunnel junction with a resistive electrode. V_n and b_n are, respectively, the dc and ac (frequency ω) voltages across the nth element, whose resistance is $R_n = V_n/I_n$ and differential resistance is $D(V_n) = (dV/dI)_{V_n} = b_n/i_n$.

tion voltage, where $\Delta(V)$ is the differential resistance of an "ideal" junction similar to the one whose conductance we wish to calculate except, of course, that in this ideal junction the electrode resistance is negligible. The difference between $\sigma(V)$ and $[\Delta(V)]^{-1}$ lies in the contribution which the finite electrode resistance makes to the former.

The procedure, which is iterative and numerical, is to compute $B_\omega(V)$, which is the rms value of $b_1(V_1)$ evaluated at the bias voltage V, in terms of $\Delta(V)$, r_E, and N. First we compute the bias in each element of the model junction. To do this we need the resistive characteristic of the ideal elemental junctions: $R(V) = V/\int_0^v dV'/D(V')$. The nth intercalated resistance element then has a voltage drop

$$V_{n+1} - V_n = r \sum_{j=1}^{n} \frac{V_j}{R(V_j)}. \qquad (1)$$

Since $V = V_1$ is the measured polarization voltage of the junction, we can then determine all the V_n and thus the differential resitance of each element, $D(V_n)$, is fixed.

We next obtain the voltage $b_1(V_1)$ for fixed bias in terms of the rms current, $i/\sqrt{2}$. Direct calculation reveals that the voltages b_n are

$$b_1 = D(V_1)i_1,$$

$$b_2 = D(V_2)i_2 = [r + D(V_1)]i_1,$$

$$b_3 = D(V_3)i_3 = r(i_1 + i_2) + D(V_2)i_2,$$

from which each partial current can be obtained as $i_n = i_1 f_n^N(V_1)/D(V_n)$, where the $f_n^N(V_1)$ depend on r as well as on the relevant subset of voltages V_j $(1 \leqslant j \leqslant n)$, where $|V_j| \geqslant |V_1|$.

We note that $f_1^N(V_1) = D(V_1)$ and although the expressions for the subsequent factors rapidly become complicated, a recursion relation exists in which the determining factors $r/D(V_n)$ can be conveniently expressed as $\rho(V_n)/(N-1)$, where $\rho(V_n) = r_E/\Delta(V_n)$. Thus if we formally define $f_0^N(V_1) \equiv N\Delta(V_1)$, we find that for $n \geqslant 2$

$$f_n^N(V_1) = f_{n-1}^N(V_1)\left(2 + \frac{\rho(V_{n-1})}{N(N-1)}\right) - f_{n-2}^N(V_1). \qquad (2)$$

We thereby obtain the total current

$$i = i_1 \sum_{n=1}^{N} \frac{f_n^N(V_1)}{N\Delta(V_n)} \qquad (3)$$

and find that the rms voltage at frequency ω is

$$B_\omega(V) = i\Delta(V)/(\sqrt{2})G_N(V), \qquad (4)$$

where

$$G_N(V) = \frac{1}{N^2} \sum_{n=1}^{N} \frac{f_n^N(V)}{\Delta(V_n)}. \qquad (5)$$

$G_N(V)$ is a converging sequence. (See Appendix.) Thus the measured conductance will be

$$\sigma(V) = G_n(V)/\Delta(V). \qquad (6)$$

EXPERIMENTAL

Junctions of Al-Al_xO_y-Bi were made and their conductance measured in order to test the model. First a strip of Al (~1000 Å) was evaporated on a glass substrate that had been prepared previously by depositing electrical contacts in the form of In dots. The Al strip was then oxidized in an O_2 glow discharge and the junction was completed by evaporating slowly a perpendicular Bi strip over the oxide. The Al used was of 99.995% purity while the Bi was 99.9999%.

Evaporations were done at pressures not higher than 4×10^{-6} Torr in a conventional liquid-N_2-trapped vacuum system. A mechanical device installed in the evaporator permits changing evaporation sources and masks without breaking the vacuum; thus a very high percentage of usable junctions was obtained.

In each case two junctions were prepared using the same oxidized Al strip. In one series of junctions the Bi layers of the two mate junctions were evaporated to different thickness; the thick-film junction (~15 000 Å), having negli-

Downloaded 18 Apr 2005 to 132.239.73.201. Redistribution subject to AIP license or copyright, see http://jap.aip.org/jap/copyright.jsp

gible electrode resistance, was used to determine $\Delta(V)$, from which $\sigma(V)$ of the thin-film mate (~ 1000 Å) could be calculated and compared with experiment. Unfortunately, slight differences in the oxides of the two mate junctions may result in important differences in their respective pseudobarriers[18] and corresponding discrepancies between the measured and calculated $\sigma(V)$.

Another series of junctions was designed to obviate this difficulty. One of the mate junctions was used as a control whereas the other, with a thin Bi film, was used to determine $\sigma(V)$. Subsequently a narrow shorting strip of Ag was evaporated over the Bi film of this junction and $\Delta(V)$ measured. Of course small modifications of the junction while evaporating the Ag might result in discrepancies between the experimental and calculated conductance.

In the third group of junctions, the Bi films of both mates were shorted with Ag overlayers and an external variable resistance was placed between them to simulate in a rudimentary way the effect of film resistance. This case would correspond to $N = 2$ in a the model calculation, with the difference that the two elemental junctions may not have identical spectra. We find that the resultant differential conductance is

$$\sigma(V) = [\Delta_1(V) + \Delta_2(V') + R_x]/\Delta_1(V)\Delta_2(V'), \tag{7}$$

where $\Delta_1(V)$ and $\Delta_2(V)$ are the differential resistances of the two junctions, R_x is the intercalated external resistance, and $V' = V[1 + R_x/R_1(V)]$.

Measurements were made at 77 K because we are primarily interested in gross changes in the conductance brought about by film resistance. The differential conductance was determined using a previously described circuit[19] based on that of Ref. 14, in which $\sigma(V)$ is determined to better than one part in 10^3, the sensitivity being about two orders of magnitude better.

RESULTS

The Al-Al_xO_y-Bi junctions made to test the model had characteristics that fell into three classes. Most were initially "well formed," which by our definition means that the conductance at 77 K resembles the letter W with well-defined peak and valleys. Room-temperature annealing of several hours in vacuum did not significantly modify the normalized conductance.

Other junctions initially showed poorly defined features (see Fig. 3). These features always sharpened after room-temperature vacuum annealing of up to 3 h, acquiring the W form, and additional annealing did not further change the normalized conductance. These junctions, once annealed, were thus also considered to be well formed. (Bi film resistance at 77 K did not vary signficantly and consistently in consequence of the annealing.)

A third class of junctions, less than 5% of those fabricated, showed two local conductance maxima within an overall "U". These junctions were not studied further.

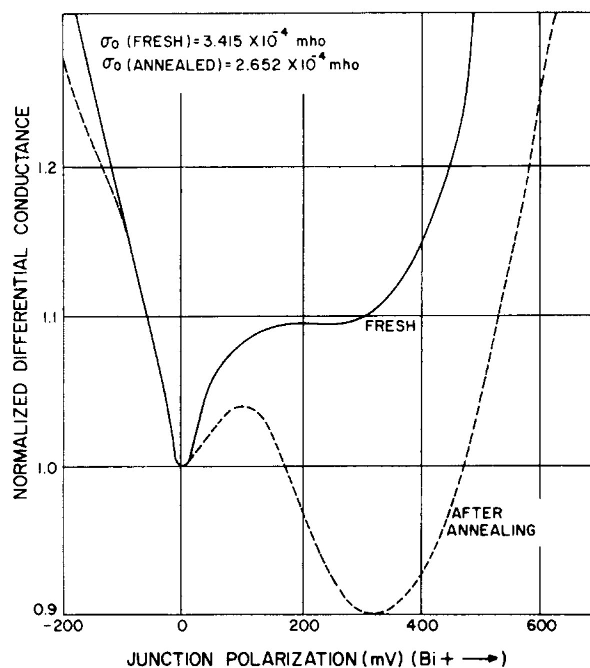

FIG. 3. Effect of annealing on Al-Al_xO_y-Bi junction whose conductance at 77 K initially lacked sharply defined features. Three hours of room-temperature annealing in vacuum significantly sharpens the structure and further annealing does not alter the normalized conductance.

Evidence exists that Bi grains formed by evaporation on mica and glass substrates tend to orient their trigonal axes perpendicular to the substrate,[5,6,8,20] and it may be that the well-formed junctions are those in which the Bi grains are predominantly in this orientation, a possibility which is consistent with the above observations.

The model was tested with well-formed junctions. As explained in the Experimental section, junctions were made in three different series, each having advantages and disadvantages. In Figs. 4–6 an example from each type of test is presented. The way in which electrode resistance distorts tunneling conductance is evident and we conclude that the model developed here satisfactorily accounts for the distortion.

In addition to examining individual cases it is important to investigate the overall consistency of the data. If we use $\rho(0) = r_E/\Delta(0)$ as the single parameter characterizing a junction, the results from about 25 paired junctions can be summarized as follows.

In junctions having $\rho(0) = 0$ the voltage at which the displaced conductance valley occurs is well defined at $V_\downarrow = 364.5\ mV \pm 3.6\%$, where the uncertainty is given as one standard deviation. The relative conductance of this valley shows a wider variation: $\sigma(V_\downarrow)/\sigma(0) = 0.95 \pm 16\%$. By contrast the voltage at which the local maximum occurs is poorly defined: $V_\uparrow = 150\ \text{mV} \pm 23\%$. The relative height of this peak has, however, a variation similar to that of the conductance valley: $\sigma(V_\uparrow)/\sigma(0) = 1.19 \pm 15\%$. We tentatively conclude that in these junctions the conductance val-

Downloaded 18 Apr 2005 to 132.239.73.201. Redistribution subject to AIP license or copyright, see http://jap.aip.org/jap/copyright.jsp

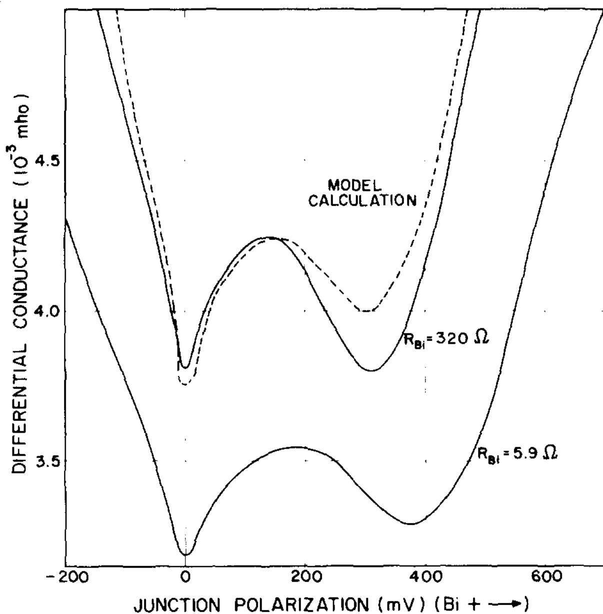

FIG. 4. Conductance of a typical pair of junctions sharing a common oxidized Al strip but differing in Bi electrode thickness. The model calculation used the thick-film junction characteristic and the electrode resistance of its thin-film mate. Small but important differences in the two pseudobarriers probably account for discrepancies between the conductance of the thin-film mate and the calculated conductance.

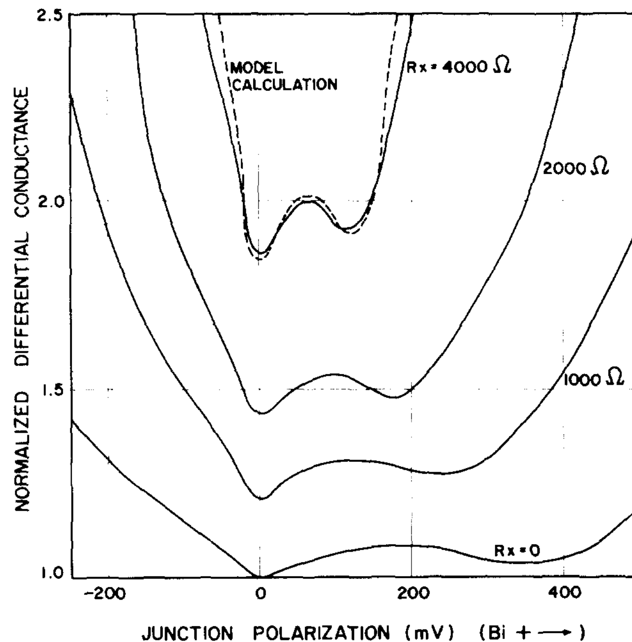

FIG. 6. Simulation of electrode resistance. A variable external resistor R_x is intercalated between a pair of junctions having shorted Bi electrodes. The model calculation for $R_x = 4000\ \Omega$ uses Eq. (7) and is based on the individual conductances (not shown) of the two junctions [$\Delta_1(0) = 2152.4\ \Omega$ and $\Delta_2(0) = 2414.7\ \Omega$].

leys (at $V = 0$,[21] and $V_\downarrow$) reflect a fundamental property of $Al\text{-}Al_xO_y\text{-}Bi$ structures, not appreciably influenced by details of junction fabrication. At the other extreme, the wide variation in $V_\uparrow$ suggests that it is determined by unknown or uncontrolled factors.

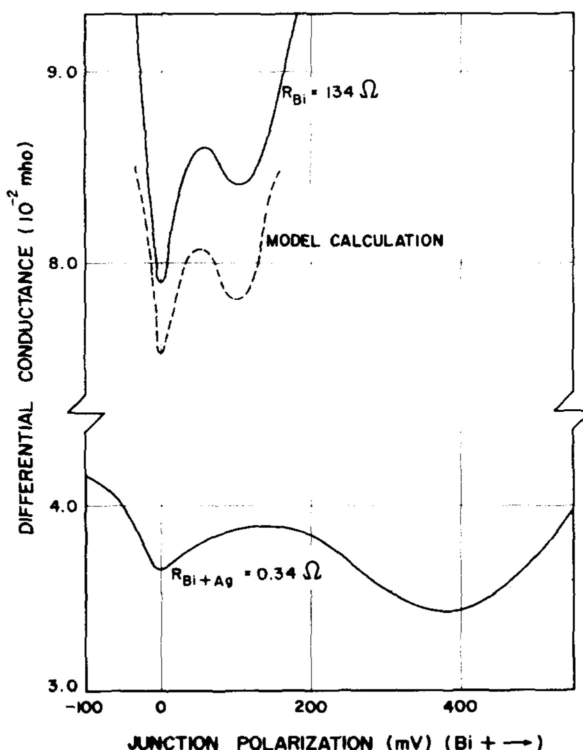

FIG. 5. Conductance of a junction before and after depositing an Ag shorting strip over the Bi electrode. Electrode resistance, as represented by the model, accounts well for the principal differences between the two curves.

Junctions were made with a maximum $\rho(0) = 10.45$. As an example of the agreement between $\sigma(V)$ calculated from the model and that measured experimentally, we mention that $V_\downarrow$ determined both ways always agrees within 4%. Typically the absolute conductance may show some discrepancy, however, probably for reasons cited in the Experimental section.

It is evident that increasing $\rho(0)$ displaces a given feature of $\sigma(V)$ to lower bias. Empirically the conductance minimum is represented by $V_\downarrow = 364.5 - 63.82\rho(0)$ mV for $0 \leqslant \rho(0) \leqslant 2$ and all data in this interval fall within $\pm 4\%$ of this line. Beyond $\rho(0) = 2$, $V_\downarrow$ continues to fall, but less rapidly; at $\rho(0) = 10$, $V_\downarrow$ has fallen by about 70%.

CONCLUSIONS

We have demonstrated that electrode resistance seriously distorts the tunneling conductance of junctions in which it is comparable with the tunneling resistance. The model proposed accounts for the variation of bias, and hence conductance, across the junction area and is not limited to small values of electrode resistance. It agrees satisfactorily with experiment in tests made with paired junctions and the results from all junctions tested are mutually consistent.

It should be noted, however, that in the present model one obtains $\sigma(V) = \sigma[r_E, \Delta(V)]$. Unfortunately, the model does not lend itself to a simple inversion, which would yield $\Delta(V) = \Delta[r_E, \sigma(V)]$, and thus permit calculating the characteristics of an ideal junction from data obtained solely on real junctions having electrode resistance.[22] Therefore it would be prudent to limit measurements to junctions in which electrode resistance is negligible or in which a good

Downloaded 18 Apr 2005 to 132.239.73.201. Redistribution subject to AIP license or copyright, see http://jap.aip.org/jap/copyright.jsp

TABLE I. Expansion coefficients a_j^n of the f_n^N.

j / n	2	3	4	5	6	7
2	1	...	...	...	...	...
3	3	1	...	...	...	...
4	6	5	1	...	...	...
5	10	15	7	1	...	...
6	15	35	28	9	1	...
7	21	70	84	45	11	1

conductor is deposited over a resistive electrode. In the junctions considered here, if the displacement of the conductance valley (V_1) is to be within one standard deviation of its position when $r_E = 0$, then the semimetal electrode resistance must be held to less than about 20% of the junction resistance [$r_E \leqslant 0.2\Delta\,(0)$].

The normalized conductance characteristic of well-formed Al-Al_x-O_y-Bi junctions is that most frequently obtained (> 95% of the junctions fabricated by our method) and in certain respects it varies remarkably little among individual junctions once electrode resistance is compensated or eliminated. Whether these highly reproducible features can be identified rigorously with bulk or surface band structure detail is beyond the scope of this work.[23] We again note that reliable calculations of tunneling conductance do not exist at present when one or both electrodes are semimetals.

ACKNOWLEDGMENTS

We wish to thank John G. Adler for valuable suggestions and Jesús L. Heiras and Miguel A. Ocampo for important contributions.

APPENDIX

We show that $G_N(V_1)$ is a converging sequence for a given polarization voltage. According to the Cauchy criterion[24] the sequence will be convergent if there exists an $\epsilon(M)$ such that for $N > M$,

$$|G_{N+1}(V_1) - G_N(V_1)| < \epsilon(M), \tag{A1}$$

where $\epsilon(M) \to 0$ as $M \to \infty$.

The expression in Eq. (A1) which must be bounded can be written explicitly as

$$\frac{1}{(N+1)^2}\left(\frac{f_{N+1}^{N+1}(V_1)}{\Delta\,(V_{n+1})} - \frac{2N+1}{N^2}\sum_{n=1}^{N}\frac{f_n^N(V_1)}{\Delta\,(V_n)} + \sum_{n=1}^{N}\frac{f_n^{N+1}(V_1) - f_n^N(V_1)}{\Delta\,(V_1)}\right), \tag{A2}$$

the structure of which can be elucidated if we neglect variations among the $\Delta\,(V_n)$. Experimentally we note that $\Delta\,(V)$ varies by a factor of less than 3 in the limited polarization range considered here, -300 to $+800$ mV. Hereafter Δ will refer to any $\Delta\,(V_n)$ and $\rho = r_E/\Delta$.

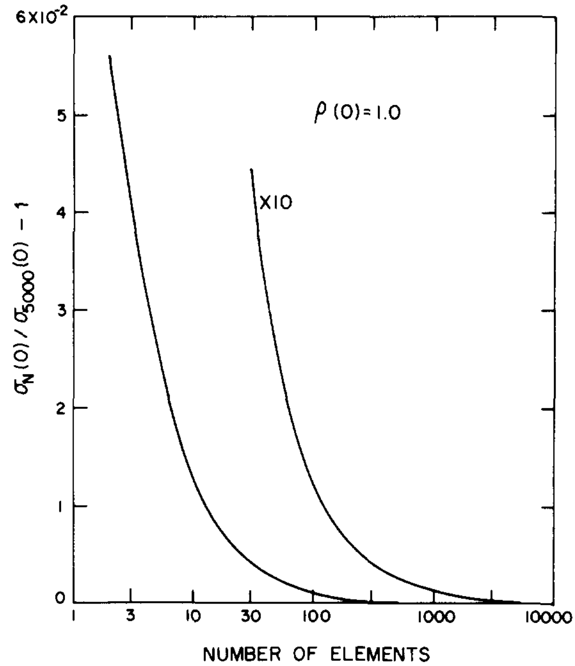

FIG. 7. Convergence of $\sigma_N(0)$ in a junction with $\rho(0) = 1$. The bias at which conductance feautures occur shows the same dependence on N as $\sigma_N(0)$.

Using the recursion relation [Eq. (2)], we are now in a position to express the factors f as follows:

$$f_1^N = N\Delta,$$

$$f_2^N = N\Delta\,[1 + \rho/N(N-1)],$$

$$f_n^N = N\Delta\left[1 + a_2^n\frac{\rho}{N(N-1)} + a_3^n\left(\frac{\rho}{N(N-1)}\right)^2 + \cdots + a_n^n\left(\frac{\rho}{N(N-1)}\right)^{n-1}\right], \tag{A3a}$$

and similarly

$$f_n^{N+1} = (N+1)\Delta\left[1 + a_2^n\frac{\rho}{N(N+1)} + a_3^n\left(\frac{\rho}{N(N+1)}\right)^2 + \cdots + a_n^n\left(\frac{\rho}{N(N+1)}\right)^{n-1}\right], \tag{A3b}$$

where the a_j^n are numerical factors, examples of which are given in Table I.

The limiting behavior of each term within the brackets of (A2) can now be obtained in a straightforward manner. The first term is

$$f_{N+1}^{N+1}/\Delta \to N\,[1 + \theta(1/N^2)], \tag{A4a}$$

where $\theta(1/N^2)$ represents terms of order N^{-2}. Secondly,

$$\begin{aligned}\frac{2N+1}{N^2}\sum_{n=1}^{N}\frac{f_n^N}{\Delta} &= \frac{2N+1}{N}\left\{1 + \left(1 + a_2^2\frac{\rho}{N(N-1)}\right) + \cdots + \left[1 + a_2^N\frac{\rho}{N(N-1)} + \cdots + a_N^N\left(\frac{\rho}{N(N-1)}\right)^{N-1}\right]\right\}\\ &= \frac{2N+1}{N}\left[N + \frac{\rho}{N(N-1)}\sum_{n=2}^{N}a_2^n + \left(\frac{\rho}{N(N-1)}\right)^2\sum_{n=3}^{N}a_3^n + \cdots + a_N^N\left(\frac{\rho}{N(N-1)}\right)^{N-1}\right]\\ &= \frac{2N+1}{N}\left(N + \tfrac{1}{6}(N+1)\rho + \frac{1}{120}\,\frac{(N+2)(N+1)(N-2)}{N(N-1)}\rho^2 + \cdots\right).\end{aligned}$$

Downloaded 18 Apr 2005 to 132.239.73.201. Redistribution subject to AIP license or copyright, see http://jap.aip.org/jap/copyright.jsp

Here we have used the fact that $a_2^n = \frac{1}{2}n(n-1)$ and $a_3^n = a_3^{n-1} + \frac{1}{6}n(n-1)(n-2)$ and the following relations[25]:

$$\sum_{n=2}^{N} a_2^n = \tfrac{1}{6}(N+1)N(N-1),$$

$$\sum_{n=3}^{N} a_3^n = \tfrac{1}{6}\sum_{n=3}^{N} \frac{n!(N+1-n)}{(n-3)!} = \frac{1}{120}(N+2)(N+1)N(N-1)(N-2).$$

Thus

$$\frac{2N+1}{N^2}\sum_{n=1}^{N}\frac{f_n^N}{\Delta} \rightarrow 2N\,[1+h_1(\rho)], \tag{A4b}$$

where $h_1(\rho) \rightarrow \frac{1}{6}\rho + \rho^2/120 + \dots$. Finally, the third term in (A2) is

$$\begin{aligned}\sum_{n=1}^{N}\frac{f_n^{N+1}-f_n^N}{\Delta} &= 1 + \left[(N+1)\left(1 + a_2^2\frac{\rho}{N(N+1)}\right) - N\left(1 + a_2^2\frac{\rho}{N(N-1)}\right)\right] + \cdots + \left\{(N+1)\left[1 + a_2^N\frac{\rho}{N(N+1)} + \cdots\right.\right.\\ &\quad \left. + a_N^N\left(\frac{\rho}{N(N+1)}\right)^{N-1}\right] - N\left[\left(1 + a_2^N\frac{\rho}{N(N-1)}\right) + \cdots + a_N^N\left(\frac{\rho}{N(N-1)}\right)^{N-1}\right]\Bigg\}\\ &= N - \frac{\rho}{N(N-1)}\sum_{n=2}^{N} a_2^N - \frac{\rho^2(3N-1)}{N^2(N+1)(N-1)^2}\sum_{n=3}^{N} a_3^n + \cdots\\ &= N - \frac{\rho}{6}(N+1) - \frac{1}{120}\frac{(3N-1)(N+2)(N-2)}{N(N-1)}\rho^2 + \cdots \rightarrow N\,[1+h_2(\rho)],\end{aligned} \tag{A4c}$$

where $h_2(\rho) \rightarrow -\frac{1}{6}\rho - \frac{1}{40}\rho^2 - \dots$.

Combining Eqs. (A4) we find that in the limit

$$|(\mathrm{A2})| \rightarrow \frac{1}{N}[h_2(\rho) - 2h_1(\rho)] \rightarrow \frac{\rho}{2N}\left(1 + \frac{\rho}{12} + \cdots\right) \tag{A5}$$

and thus if we choose $\epsilon(M) = \rho(1 + \frac{\rho}{12} + \dots)/2M$ we will have satisfied the Cauchy condition. Of course the speed with which convergence is attained will in a given case depend on the subset of factors $[\rho(V_n)]$ which intervene in the calculation of $G_N(V_1)$.

In junctions of the type considered here we find that if $\rho(0)$ is 1.0, a model of $N \sim 200$ elements determines $\sigma(V)$ to within 0.1% of its asymptotic form, in practice estimated from the results for $N = 5000$. For a precision of 1% one needs only ~ 20 elements. In Fig. 7 we show the convergence of $\sigma(0)$ in function of N for one junction. In this work $\sigma(V)$ was calculated to a precision of at least 0.05%.

[1] S. Mase, J. Phys. Soc. Jpn. **13**, 434 (1958); **14**, 584 (1959).
[2] S. Golin, Phys. Rev. **166**, 643 (1968).
[3] J. J. Hauser and J. R. Testardi, Phys. Rev. Lett. **20**, 12 (1968).
[4] J. R. Vaisnys, D. B. McWhan, and J. M. Rowell, J. Appl. Phys. **40**, 2623 (1969).
[5] Y. Sawatari and M. Arai, J. Phys. Soc. Jpn. **28**, 360 (1970).
[6] G. A. Mironova, Ya. G. Ponomarev and L. Roshta, Sov. Phys. Solid State **17**, 574 (1974).
[7] J. Straus and J. G. Adler, Solid State Commun. **15**, 1639 (1974).
[8] H. T. Chu, N. K. Eib, and P. N. Henriksen, Phys. Rev. B **12**, 518 (1975).
[9] H. T. Chu, N. K. Eib, P. N. Henriksen, and S. M. Steele, Phys. Rev. B **18**, 4546 (1978).
[10] L. Esaki and P. J. Stiles, Phys. Rev. Lett. **14**, 902 (1965); **16**, 574 (1966).
[11] D. J. BenDaniel and C. B. Duke, Phys. Rev. **160**, 679 (1966).
[12] See, for example, M. A. Belogolovskii, A. A. Galkin, and V. M. Svistunov, Sov. Phys. JETP **42**, 912 (1975).
[13] I. Giaever has noted that electrode resistance affects measured junction resistance and he has presented an expression for the effect which, however, does not take into account the variation of conductance across the area of the junction ["*Tunneling Phenomena in Solids*", edited by E. Burstein and S. Lundqvist (Plenum, New York, 1969), p. 27,28]. Chu *et al.* made use of this correction formula in Ref. 9.
[14] J. G. Adler and J. E. Jackson, Rev. Sci. Instrum. **37**, 1049 (1966).
[15] A. F. Hebard and P. W. Shumate, Rev. Sci. Instrum. **45**, 529 (1974).
[16] S. Colley and P. Hansma, Rev. Sci. Instrum. **48**, 1192 (1977).
[17] J. G. Adler, T. T. Chen, and J. Straus, Rev. Sci. Instrum. **42**, 362 (1971).
[18] W. F. Brinkman, R. C. Dynes, and J. M. Rowell, J. Appl. Phys. **41**, 1915 (1970).
[19] T. A. Will and J. L. Heiras, Rev. Mex. Fis. **23**, FA39 (1974).
[20] Yu. F. Komnik and E. I. Bukhshtab, Sov. Phys. JETP **27**, 34 (1968).
[21] The "zero bias" valley always occurs precisely at $V = 0$.
[22] After the authors submitted this article, they became aware of work by J. W. Osmun which treats the problem of electrode resistance in the normalization of superconductive tunneling spectra [Phys. Rev. B **21**, 2829 (1980)]. Osmun emphasizes the bias dependence of the correction for electrode resistance and he presents an inversion scheme giving (in our notation) $\Delta(V)$ as an expansion in powers of r_E, valid when $\rho(V) \ll 1$.
[23] We have fabricated a small number of junctions of the types Bi-Bi_xO_y-M, where $M =$ Bi and Al. At 77 K the conductance of such junctions is highly symmetrical and no indication of structure is visible to the bias limit tested, $\pm$ 600 mV. We believe that the semimetal oxide interfaces are crucial in determining tunneling conductance. See also Ref. 7.
[24] R. Courant, *Differential and Integral Calculus* (Interscience, New York, 1954), Vol. 1, p. 367.
[25] I. S. Gradshteyn and I. M. Ryzhik, *Table of Integrals, Series and Products* (Academic, New York, 1965) p. 1 and 3.

Downloaded 18 Apr 2005 to 132.239.73.201. Redistribution subject to AIP license or copyright, see http://jap.aip.org/jap/copyright.jsp